Determination of rain age via γ rays from accreted radon progeny

Determination of rain age via γ rays from accreted radon progeny

M. B. Greenfield,[1,a)] N. Ito,[1] A. Iwata,[1] K. Kubo,[1] M. Ishigaki,[1] and K. Komura[2]
[1]*International Christian University, Mitaka, Tokyo 1818585, Japan*
[2]*Low Level Radioactivity Laboratory, Kanazawa University, Ishikawa 923122, Japan*

(Received 19 June 2008; accepted 12 August 2008; published online 8 October 2008)

The relative γ ray activities from ^{214}Pb and ^{214}Bi condensed from precipitation are used to determine its "age," the average time the accreted activity has been removed from secular equilibrium. A verifiable assumption that radon progeny on/in the surface/volume of droplets mostly remains in secular equilibrium until they begin their descent, enables estimates of their transit times to ground of typically a few tens of minutes. This agrees well with the time expected for the activity on the surface of droplets to reach the ground from heights of a few kilometers. The half lives of γ activities from ^{214}Bi and ^{214}Pb, 19.7 and 26.9 min, respectively, are on the same scale as transit time to ground and close enough to each other to measure ratios of activities from secular equilibrium (1.00) to transient equilibrium (3.88) within a few hundreds of minutes. The ratio of γ count rates is independent of knowledge of either initial activity or any systematic errors and thus limited only by the uncertainty from counting statistics, which from condensates of 5–30 l of rain viewed with 2π solid angle by a 50% efficient, high-resolution Ge detector is only a few percent. These ratios fit extremely well to known theoretical curves, which cannot only be used to date rain but can also be extrapolated backward to determine radon progeny activities in rain prior to its descent, knowledge of which may facilitate further studies using radon progeny as tracers. © *2008 American Institute of Physics*. [DOI: 10.1063/1.2990773]

I. INTRODUCTION

The goals of this work include (1) measurements of the mean "age" of a volume of precipitation collected at ground level using γ activities of atmospheric radon progeny as tracers, (2) determination of the initial activity/volume within precipitation, and (3) comparison of the mean age of precipitation with the time it takes droplets to fall from clouds of a few kilometers with expected terminal speeds. Reliable, reproducible, and statistically significant radiometric dating of the age of activity on/in rain and snow is used to estimate the time that activity attached to the rain or snow has been removed from secular equilibrium until it reaches the collection point at ground level. Ages are estimated via measurement of the transition of the relative γ ray rates (GRRs) from ^{214}Pb and ^{214}Bi, attached primarily to the surface of droplets, from secular to transient equilibrium. Since the transit times of precipitation cannot be less than its age, then the latter may be used to determine a lower limit on the former.

This work, consistent with earlier work, suggests that the preponderant accretion of activity is adsorbed on the surface of rain drops in its formation prior to its descent toward the ground, rather than via scavenging.[1,2] Thus herein measured ages of a few tens of minutes may provide useful estimates of the average precipitation transit times and not just their upper limits.

Estimates of average fall velocities of rain from heights of a few kilometers based upon this assumption agree very well with terminal velocities calculated for various drop size distributions.[3–8] There is a paucity of reliable data to test models for the formation, velocity, and transit times of rain because they are difficult to measure.[9–12] Existing models refer to the distribution of terminal velocities of individual droplets relative to their size/shape (see Fig. 1), whereas we actually measure the weighted mean velocity of surface activity, which may be correlated with the mean and standard deviation of the velocity of rain in its entirety [refer to Eqs. (14), (15), (17), and (18) in Sec. II), all of which are functions of rainfall rate. The method presented and data thus obtained herein will most likely become invaluable tools for understanding precipitation and cloud formation.

Relative background subtracted GRRs from ^{214}Pb (GRR_{Pb}) and ^{214}Bi (GRR_{Bi}) condensed from rain collected at ground level can be used to determine age because the ratio of their two activities, A_{Pb}/A_{Bi}, within a given sample as a function of time depends only upon their well known decay constants. The beauty of this relative measurement is that

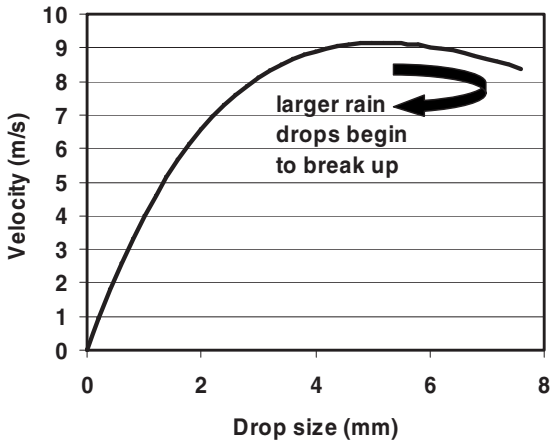

FIG. 1. Velocity vs drop size distribution.

[a)]Electronic mail: greenfield@icu.ac.jp.

absolute initial activities need not be known and the ratio of A_{Pb}/A_{Bi} is independent of sample size, sample preparation method or time, solid angle, or any other systematic or unknown errors in the measurement procedure. Since the ratio $A_{Bi}(t)/A_{Pb}(t)$ is by definition equal to one at secular equilibrium and since it evolves toward an inevitable and precisely calculable transient equilibrium of 3.88, the precision in dating rain depends only on the statistical accuracy with which $GRR_{Bi}(t)/GRR_{Pb}(t)$ can be determined [see Sec. II Eq. (11)].

The remarkably large initial activities of $A_{Pb}(t=0)$ and $A_{Bi}(t=0)$ determined from the activity in the collected rain water are sufficient to follow the ratio of these activities for several of their half lives, 19.9 and 26.8 min, respectively, to within 1%–10%. These half lives are fortuitously on the same time scale as the precipitation events being monitored. Since ^{214}Pb decays into ^{214}Bi, and since the difference in their half lives (6.9 min) is fortuitously small, transition from secular to transient equilibrium occurs within a few 100 min (see Sec. II). In order to maximize statistics in measuring $GRR_{Bi}(t)/GRR_{Pb}(t)$ over a few half lives ion exchange resins are used to condense the ^{214}Pb and ^{214}Bi ions from tens of liters of collected rain water.

Since $A_{Bi}(t)/A_{Pb}(t)$ is proportional to $GRR_{Bi}(t)/GRR_{Pb}(t)$ and is theoretically determinable for all values of t, including $t=0$, fitting the measured $GRR_{Bi}(t)/GRR_{Pb}(t)$ to $A_{Bi}(t)/A_{Pb}(t)$ enables precise determination of $A_{Bi}(t=0)/A_{Pb}(t=0)$ without making measurements at $t=0$. Further if one can estimate the relative energy dependent efficiencies, solid angle, and degree to which the activity in rain water is condensed within prepared samples, one can also make absolute estimates of both $A_{Bi}(t=0)$ and $A_{Pb}(t=0)$.

Measurements of atmospheric GRR at International Christian University[13] (ICU) began shortly after a nuclear accident in Tokaimura, Japan in 1999. A diurnal cycle of exhaled radon and its progeny gives rise to a diurnal cycle of atmospheric GRR, which at ground level has measured amplitude on the same order of magnitude as the background from all other sources combined.[13] This activity peaks just before sunrise and is then largely carried to higher elevations via vertical convective and turbulent transport of the vapor and/or particulate matter to which it is attached. This cycle of exhaled radon progeny is the source of the GRR that we use as a natural tracer of precipitation, yet atmospheric GRR from this cycle can mostly be eliminated as a source of background when measurements are made above about 15 m rather than at ground level.[1] In earlier work increases in the background subtracted atmospheric GRRs during precipitation, measured on the rooftop of the ICU Natural Science building and at three other locations in Japan, with NaI scintillation detectors and/or Ge detectors, have been observed.[1] Gamma ray energies are cleanly identifiable as from radon progeny, which have attached to water droplets that have returned to ground level. A model applied to all data obtained in Japan[1,13] as well as data from New Zealand[14] and the USA (Ref. 15) has established that accreted activity is largely adsorbed on the surface with a lesser amount absorbed within the volume of raindrops, and suggests that this activity is in secular equilibrium until the rain drop begins its descent[1] [see Eq. (16) of Sec. II].

Small cloud droplets have terminal velocities of a few hundredths of m s^{-1}, but are kept aloft by vertical air currents. Smaller droplets coalesce into larger droplets with increasing terminal velocities and eventually catch up and merge with others. Raindrops are formed from millions of cloud droplets attaining sizes of a few millimeters up to about 5–7 mm before air resistance deforms them[16–18] and disintegrates them[17–19] into smaller raindrops once again (see Fig. 1).[8] Observations in this and previous work are consistent with a model assuming that most of the activity is adsorbed on, and thus proportional to, the collective surface area of droplets during their formation, and that it mostly remains in secular equilibrium until the droplet is large enough to begin its journey earthward.[1,2] Although scavenging of further activity cannot be ruled out, it is found not to be significant. Drop size distributions as a function of rain rate[6,20–24] and terminal velocity as a function of drop size[9–12] have been measured and parametrized.[3–8,25–27] However, the data herein, obtained using radiometric tracers, may be invaluable in determination of average transit times and velocities *in situ*.

Absolute activities from radon progeny in the upper atmosphere in general, and within rain clouds and on precipitants in particular, are estimated for each precipitation event and occur within a surprising large range of a few $Bq\ l^{-1}$. These estimates may be used as a base line for further radiometric studies using natural radon progeny as tracers. These data, along with measurements of atmospheric GRR which establish the degree to which activity is adsorbed/absorbed on/within rain droplets and radiometric rain rates[1] may be proven sufficient to set many models to the test. The theoretical bases for analyses of data are described in Sec. II, experimental method in Sec. III, data and analyses in Sec. IV, and summary in Sec. V.

II. THEORY

In this work we focus on ^{214}Pb which decays with a 26.8 min half life into ^{214}Bi which itself then decays with a 19.9 min half life. They are progeny of radon gas which comes from the ^{238}U ($t_{1/2}=4.5\times10^{9}$ yr) decay chain, which is exhaled from the earth, and which is thus found in the atmosphere. Radon does not adhere to the precipitants, and the half life of ^{218}Po is sufficiently short such that it is effectively removed after secular equilibrium is broken. The half lives of ^{214}Bi and ^{214}Pb are on the same scale as precipitation events, and thus are ideal for monitoring. The ^{214}Bi and ^{214}Pb γ counting rates as a function of time, $GRR_{Bi}(t)$ and $GRR_{Pb}(t)$, enable determinations of rain age without any measurements of the initial activity within precipitation, the detector geometry or efficiency, or any systematic errors in the experiment. This is because their relative activities evolve from that of secular equilibrium $[A_{Bi}(0)/A_{Pb}(0)=1]$ to transient equilibrium $[A_{Bi}(t)/A_{Pb}(t)=3.883]$ in a precisely predictable and in this case relatively short time because their half lives differ by only 6.8 min. The activity for ^{214}Pb

is by definition a constant while in secular equilibrium with its decay chain, but as soon as it is removed from secular equilibrium ($t=0$) it decays as[28]

$$A_{\mathrm{Pb}}(t) = A_{\mathrm{Pb}}(0)e_1^{-\lambda t} = \lambda_1 N_{\mathrm{Pb}}(0)e_1^{-\lambda t}, \tag{1}$$

where λ_1 is the decay constant for ^{214}Pb$=\ln 2/(t_{1/2})$ $=0.025\ 86\ \mathrm{min}^{-1}$ and $N_{\mathrm{Pb}}(0)$ is the number of ^{214}Pb at $t=0$. Similarly if, and only if, ^{214}Bi was isolated from its parent, ^{214}Pb, then it would decay as

$$A_{\mathrm{Bi}}(t) = A_{\mathrm{Bi}}(0)e_2^{-\lambda t} = \lambda_2 N_{\mathrm{Bi}}(0)e_2^{-\lambda t}, \tag{2}$$

where λ_2 is the decay constant for ^{214}Bi$=\ln 2/(t_{1/2})$ $=0.034\ 83\ \mathrm{min}^{-1}$. Until $t=0$ they are in secular equilibrium and by definition have identical activities,

$$A_{\mathrm{Bi}}(0) = \lambda_2 N_{\mathrm{Bi}}(0) = \lambda_1 N_{\mathrm{Pb}}(0) = A_{\mathrm{Pb}}(0),$$

and thus

$$N_{\mathrm{Bi}}(0) = N_{\mathrm{Pb}}(0)\lambda_1/\lambda_2 = 0.726 N_{\mathrm{Pb}}(0). \tag{3}$$

However as soon as these two isotopes are removed together from secular equilibrium, then ^{214}Pb decays into ^{214}Bi at the rate given by Eq. (1), but the number of ^{214}Bi has two components,

$$N_{\mathrm{Bi}}(t) = (\lambda_1/\lambda_2)N_{\mathrm{Pb}}(0)e_2^{-\lambda t} + N_{\mathrm{Pb}}(0)[\lambda_1/(\lambda_2-\lambda_1)](e_1^{-\lambda t} - e_2^{-\lambda t}), \tag{4}$$

the first of which represents the decay of the activity of ^{214}Bi present at time $t=0$ as per Eq. (2), and the second term, the decay of the ^{214}Bi that is being fed by ^{214}Pb.

At time $t=0$ Eq. (4) is identical to Eq. (3). Further we can find $A_{\mathrm{Bi}}(t)$

$$A_{\mathrm{Bi}}(t) = \lambda_1 A_{\mathrm{Pb}}(0)e_2^{-\lambda t} + A_{\mathrm{Pb}}(0)[\lambda_1\lambda_2/(\lambda_2-\lambda_1)](e_1^{-\lambda t} - e_2^{-\lambda t}), \tag{5}$$

and then the ratio of the two activities:

$$A_{\mathrm{Bi}}(t)/A_{\mathrm{Pb}}(t) = e_2^{-\lambda t}/e_1^{-\lambda t} + [\lambda_2/(\lambda_2-\lambda_1)](e_1^{-\lambda t} - e_2^{-\lambda t})/e_1^{-\lambda t}. \tag{6}$$

Since $\lambda_2 > \lambda_1$, then $e_1^{-\lambda t}$ becomes much greater than $e_2^{-\lambda t}$ as time progresses toward infinity (in this case just a few 100 min) and Eq. (5) simply reduces to

$$\lambda_2/(\lambda_2-\lambda_1) = 3.883. \tag{7}$$

Neither the ratio of activities at time $t=0$, secular equilibrium Eq. (3), or at $t=\infty$, transient equilibrium Eq. (7), are subject to any systematic errors. Furthermore, we may lump the product of the ratios of energy dependent detection efficiencies $(\varepsilon_1/\varepsilon_2)$, branching ratios (b_1/b_2) of the chosen peaks, and the unknown fractions (f_1/f_2) of each isotope coagulated from rain $(\varepsilon_1 b_1 f_1/\varepsilon_2 b_2 f_2)$ into one overall normalization constant, C^*, which may then be factored out,

$$C^*[\mathrm{GRR}_{\mathrm{Bi}}(t)/\mathrm{GRR}_{\mathrm{Pb}}(t)] = A_{\mathrm{Bi}}(t)/A_{\mathrm{Pb}}(t), \tag{8}$$

$$C^*[\mathrm{GRR}_{\mathrm{Bi}}(t=0)/\mathrm{GRR}_{\mathrm{Pb}}(t=0)] = A_{\mathrm{Bi}}(0)/A_{\mathrm{Pb}}(0) = 1, \tag{9}$$

$$C^*[\mathrm{GRR}_{\mathrm{Bi}}(t_\infty)/\mathrm{GRR}_{\mathrm{Pb}}(t_\infty)] = A_{\mathrm{Bi}}(t_\infty)/A_{\mathrm{Pb}}(t_\infty) = 3.88 \tag{10}$$

Dividing Eq. (9) by Eq. (8) we get

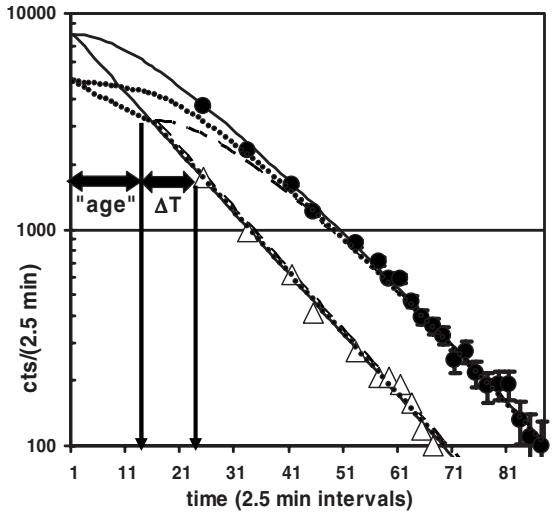

FIG. 2. ^{214}Bi (609 keV filled circles) and ^{214}Pb (352 keV open triangles) γ ray count rates as a function of 2.5 min bin intervals taken on 25 April 2006, and decay curves for breaking of secular equilibrium at the beginning of fall (solid lines), at the beginning of collection (dashed lines), and at the beginning of each 2.5 min interval. The double headed arrows indicate the rain age and sample preparation time from left to right, respectively.

$$[\mathrm{GRR}_{\mathrm{Bi}}(t=t_{\mathrm{long}})/\mathrm{GRR}_{\mathrm{Pb}}(t=t_{\mathrm{long}})]/[\mathrm{GRR}_{\mathrm{Bi}}(t=0)/\mathrm{GRR}_{\mathrm{Pb}}(t=0)] = 3.88. \tag{11}$$

In fact GRR at $t=0$ cannot be measured at ground and the counting statistics as t approaches t_∞ will be poor. However, if we define t_i as time between the breaking of secular equilibrium and the weighted mid point of the initial data interval, ΔT_{meas} typically 5–10 min, then $t_n = t_i + n\Delta T_{\mathrm{meas}}$ is the weighted midtime (the activity is decaying within the interval it is being measured) for the nth data interval, from $t=t_i$ to about $t>200$ min. Then t_i and C^* may be determined by a two parameter fit of $\mathrm{GRR}_{\mathrm{Bi}}(t_n)/\mathrm{GRR}_{\mathrm{Pb}}(t_n)$ to Eqs. (8) and (11). The value of C^* thus obtained for the 609 keV peak of ^{214}Bi and 352 keV peak of ^{214}Pb is consistently the same and is entirely free of any and all systematic errors. The best value of t_i depends upon the sample collection and preparation time, ΔT_{prep}, for each experiment and is typically around 15–45 min. From Eq. (11) $\mathrm{GRR}_{\mathrm{Bi}}(t=0)/\mathrm{GRR}_{\mathrm{Pb}}(t=0)$ may be obtained from $\mathrm{GRR}_{\mathrm{Bi}}(t=t_{\mathrm{long}})/\mathrm{GRR}_{\mathrm{Pb}}(t=t_{\mathrm{long}})$. Since $C^* = (\varepsilon_1 b_1 f_1/\varepsilon_2 b_2 f_2)$ may thus be determined, if one empirically estimates $\varepsilon_1 b_1 f_1$ then one can determine $A_{\mathrm{Pb}}(0) = \varepsilon_1 b_1 f_1$ $\mathrm{GRR}_{\mathrm{Pb}}(t=0)$ and $A_{\mathrm{Bi}}(0) = \varepsilon_2 b_2 f_2$ $\mathrm{GRR}_{\mathrm{Bi}}(t=0)$ despite the fact that these cannot be measured directly.

In order to determine age, then ΔT_{prep}, which is the sum of time lag, sample collection and preparation times (see Sec. III) for each measurement must be subtracted from t_i obtained from the fits,

$$\mathrm{age} = t_i - \Delta T_{\mathrm{prep}}. \tag{12}$$

In Fig. 2 the ^{214}Pb and ^{214}Bi experimental activities (triangles and circles, respectively) are compared to Eqs. (1), (5), and (10) assuming the activity in the rain is either (i) completely removed from secular equilibrium at $t=0$ (solid lines), (ii) remains in secular equilibrium until it is collected (dashed lines), or (iii) is scavenged in its fall to the earth (dotted lines). The dotted curve is an average of an iterative

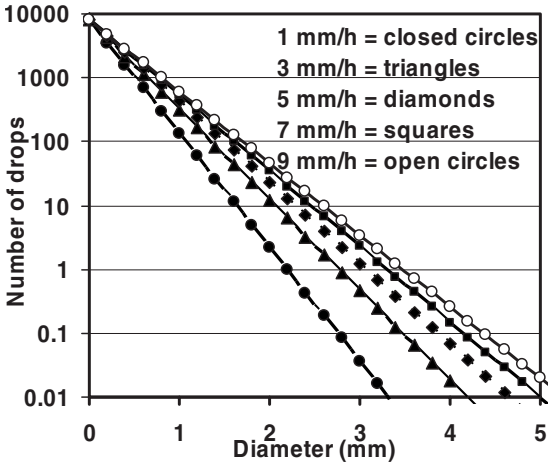

FIG. 3. Number of drops vs diameter (millimeter) and for rain rates of 1, 3, 5, 7, and 9 mm/h as the closed circles, triangles, diamonds, squares, and open circles, respectively.

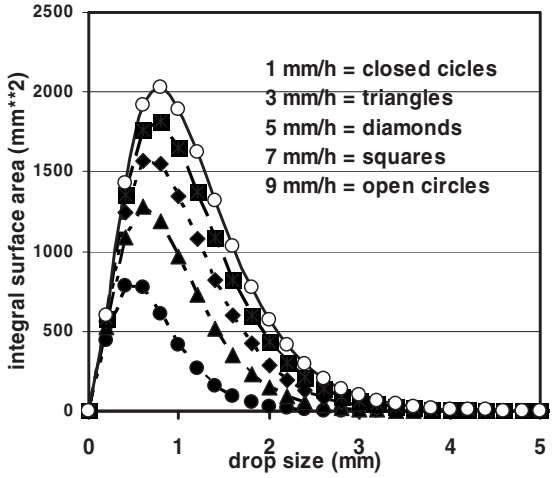

FIG. 4. Integral surface area (mm^2) vs drop size (millimeter) for rain rates of 1, 3, 5, 7, and 9 mm/h as closed circles, triangles, diamonds, squares, and open circles, respectively.

sum of Eq. (1) for ^{214}Pb or Eq. (5) for ^{214}Bi restarted at $t=0$ every 2.5 min interval. The data obtained herein are best fit by the first model (i), which is in agreement with our previous work,[1] and which along with Eq. (12) yields reasonable ages of tens of minutes.

To check whether transit velocities based upon these ages are reasonable, they may be compared to calculated terminal velocities, v_{term}, of individual rain drops. For relatively small, spherical rain drops one may apply Stokes' law[29]

$$v_{\text{term}} = \frac{2}{9}\frac{r^2 g(\rho_p - \rho_f)}{\eta}, \tag{13}$$

where g is the acceleration of gravity, ρ_p is the density of water, and ρ_f is the density of air. Larger droplets become deformed[16–18] and experience turbulence and eventually break up[16,19] such that measured v_{term} does not follow Eq. (13). Rather one must rely upon parametrizations of v_{term} versus drop size, diameter$=d$, which best fit the data of both Gunn and Kinzer[9] as well as that of Beard and Prupacher[10] by Grosh,[3] Sekhon and Srivastava,[4] Best,[5] Gossard *et al.*,[6] van Boxel,[7] or Uplinger,[8] all of which give reasonable fits, but the latter of which is illustrated in Fig. 1, is used throughout this work, and is given by

$$v_{\text{term}} = 9.65(1.0 - e^{-0.53d}). \tag{14}$$

One can also parametrize the measured drop size distribution[30] with the empirical relationship of Marshall and Palmer,[25] the latter of which is illustrated in Fig. 3 for various rain precipitation rates, is used throughout this work, and is given by

$$N(d) = N_0 e^{-\Lambda d}, \tag{15}$$

where $\Lambda = 4.1\ (\text{rain rate in mm h}^{-1})^{-0.21}$ and where $N_0 = 8 \times 10^3\ \text{m}^{-3}\ \text{mm}^{-1}$.

From earlier work[1] we determined that the observed GRRs are proportional to effective radiometric precipitation rates (RPRs) to the power α,

$$\text{GRR} = C[\text{RPR}^{\alpha}], \tag{16}$$

where α ranges between 0.4 for surface adsorption and 0.6 for volume absorption, and C is a normalization constant including experimental and systematic factors, but which only remains constant if the density of initial adsorbed/absorbed activity is relatively constant throughout a given rain event. For most of the data C remains remarkably constant and fits are obtained with α around 0.45 ± 0.05 suggesting that activity resides mostly on the surface of rain drops. This seems reasonable since (1) the ^{214}Pb and ^{214}Bi are produced via decay and, being ionized, reside on the surface of droplets due to their mutual repulsion and (2) the activity per unit mass of melted snow has about 20 times the activity per unit volume as an equivalent amount of rain water with less surface area.[13]

The age of the rain drop is determined from its accreted activity, which is thus proportional to the integral surface area of the rain drops. From the drop size distribution, see Fig. 3 and Eq. (14), the integral surface area per drop size for different RPRs may be estimated as

$$\sum_{i=1}^{n} \text{area}(d_i) = \sum_{i=1}^{n} N(d) 4\pi (d_i/2)^2 = \sum_{i=1}^{n} 4\pi (d_i/2)^2 N_0 e^{-\Lambda d}, \tag{17}$$

as shown in Fig. 4. Then one may obtain a weighted mean surface area of the average drop size as

$$\frac{\sum_{i=1}^{n} N(d)\text{area}(d_i)}{\sum_{i=1}^{n} N(d)} = \frac{\sum_{i=1}^{n} N(d) 4\pi (d_i/2)^2}{\sum_{i-1}^{n} N(d)} = \frac{\sum_{i=1}^{n} 4\pi (d_i/2)^2 N_0 e^{-\Lambda d}}{\sum_{i=1}^{n} N(d)}. \tag{18}$$

The rate at which activity falls to the ground is associated

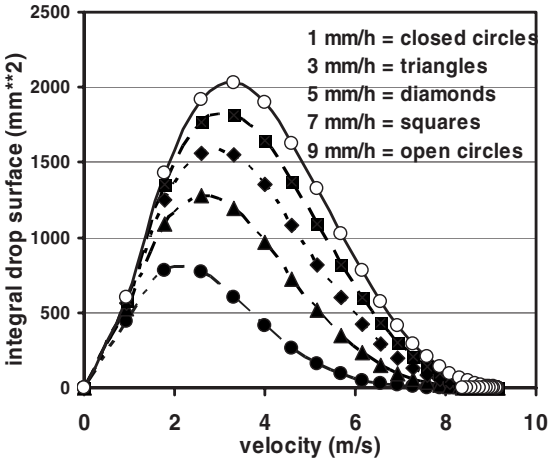

FIG. 5. Integral surface area (mm^2) versus their velocities for rain rates of 1, 3, 5, 7, and 9 mm/h as closed circles, triangles, diamonds, squares, and open circles, respectively.

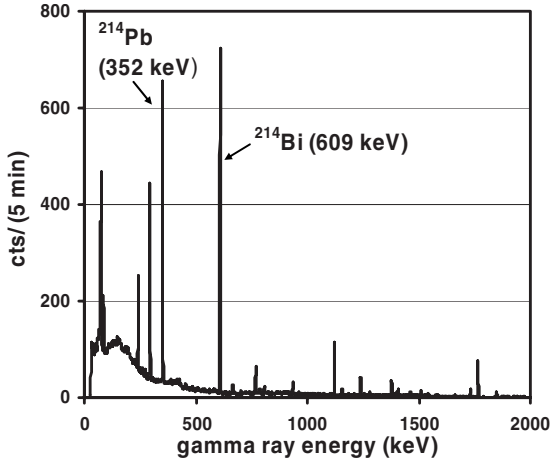

FIG. 6. Gamma ray energy spectrum for a rain sample collected on 2 May 2006.

with the weighted mean velocity of the surface area, v_{surf}, which is proportional to the square of diameter of each drop. The velocity of a given volume of rain is related to the weighted mean velocity of the volume of each drop, v_{vol}, which is proportional to the cube of the diameter. In other words, when a burst of rain with its associated velocity and size distributions given by Eqs. (14) and (15), respectively, begins its descent at time $t=0$, the mean *volume* of rain will have a greater velocity (and thus fall in less time) than the mean *surface* area, both of which fall at velocities greater than the *average* drop. Thus we find that $v_{vol} > v_{surf} > v_{drop}$ and $\Delta T_{drop} > \Delta T_{surf} > \Delta T_{vol}$. Since age is in proportion to v_{surf}, if we plot the surface weighted drop size versus its associated velocity we obtain the velocity distribution of surface versus $v(n)$, as shown in Fig. 5, from which we may obtain v_{surf} as 2.95, 3.55, 3.85, 4.05, and 4.2 m s^{-1} for rain rates of 1, 3, 5, 7, and 9 mm h^{-1}, respectively. As will be shown in Sec. IV, the data obtained yield mean ages of about 30 min, corresponding to mean velocities from about 1 to 3 m s^{-1} from an assumed range of mean falling heights of 2–5 km, in good agreement with the velocity distributions for the various precipitation rates shown in Fig. 5.

III. EXPERIMENTAL METHOD

The primary goal of this experiment is to track the time sequence of two activities $A_{Pb}(t)$ and $A_{Bi}(t)$ with half lives of 26.8 and 19.9 min, respectively, and branching ratios of 37.6% and 46.1% to states at 352 and 609 keV, respectively. These two peaks dominate all γ ray energy spectra of the activity condensed from collected rain water. Figures 6 and 7 are γ ray energy spectra of a rain sample collected during a thunderstorm on 2 May 2006, and the same sample measured about 150 min later, respectively. One can clearly see the dominance of the 351 and 609 keV lines in Fig. 6 and their reduction in activity five half lives later by about a factor of 30. The other surviving peak with constant activity is ^{40}K which is unrelated to the radon progeny.

Since 352 and 609 keV lines are measured within the same γ ray spectra, the ratio of their activities is free from all systematic errors. All other experimental parameters were set in order to optimize the amount of activity in each sample and thus the counting statistics.

Between 5 and 30 l of rain water were collected from each of two identical east and west facing roofs of the ICU science building, each with nonporous rapidly draining surfaces of 9.8 m^2. Since the activities in question have half lives on the order of 20–30 min, the collection process was halted if it took more than 20 min to double the sample size. The time lag between the incident rain and its collection, which was measured by spraying an effective rain fall rate of 5 mm h^{-1} on the roof with a hose, was found to be about 1 min for both dry and previously wetted surfaces. The typical collection times for 5–30 l of rain water per roof were around 3–13 min. The error in the water collection processes was typically less than 2 min.

Following the procedures developed at the Low Level Radioactivity Laboratory,[31] 6 g/l each of cation (POWDEX^R-PCH) and anion (POWDEX^R-PCH) ion exchange resins were added to the collected water, stirred in, and allowed to settle for approximately 3–5 min. All but about 2 l of the mixture was decanted and the last few liters containing the majority of the settled condensate was subse-

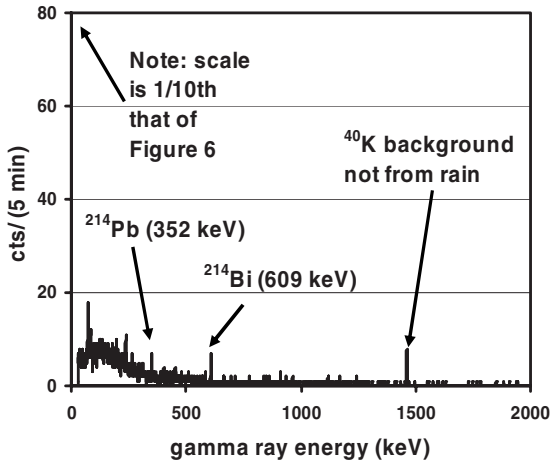

FIG. 7. Gamma ray energy spectrum for the same rain sample, as shown in Fig. 6 4 h later.

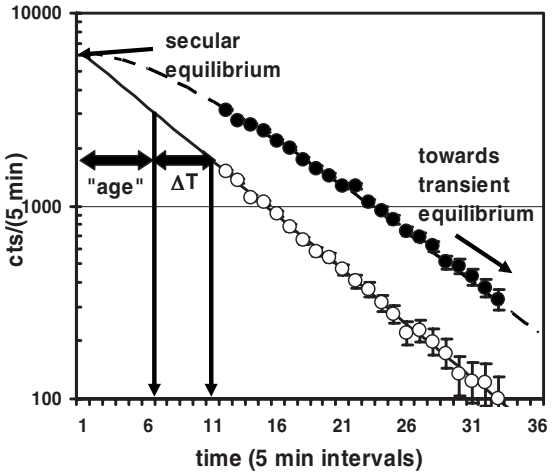

FIG. 8. ^{214}Bi (609 keV closed circles) and ^{214}Pb (352 keV open circles) γ ray count rates as a function of 5.0 min bin collection intervals from rain collected on 24 May 2006, and their theoretical decay curves assuming they are in secular equilibrium at beginning of fall as dashed and solid lines, respectively.

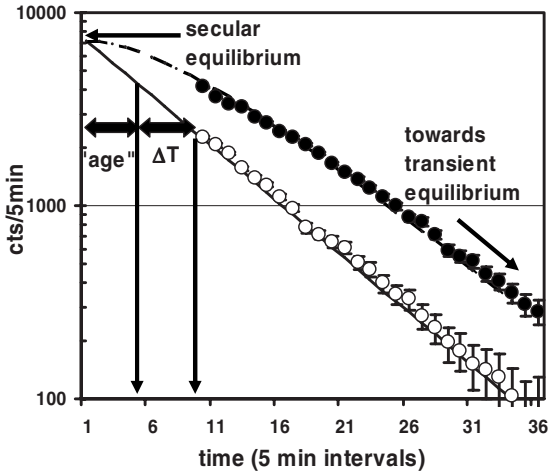

FIG. 9. ^{214}Bi (609 keV closed circles) and ^{214}Pb (352 keV open circles) γ ray count rates as a function of 5.0 min bin collection intervals from a second sample of rain collected on 24 May 2006, and their theoretical decay curves assuming they are in secular equilibrium at beginning of fall as dashed and solid lines, respectively.

quently filtered through one of two aspirators. The entire collection and preparation times were together typically 7–20 min depending on a large extent upon the sample size. The filtrate was formed into a dry cylindrical wafer of about 5 cm diameter and with thickness on the order of 1–2 cm depending upon the initial water volume and resin added. This wafer was placed in direct contact with the 5 cm diameter surface of a portable, internally cooled, 50 mm diameter by 30 mm deep High Purity Germanium (HPGe) detector.[32]

For the case of snow, the collection times were typically on the order of an hour or more. The snow was first melted prior to the addition of the ion exchange resins, but otherwise the same procedures as that for rain were followed.

A secondary goal of this experiment was to determine the absolute initial activity of each isotope within the collected rainwater. This requires knowledge of (1) the energy dependent efficiencies, (2) the relative branching ratios, (3) the fraction of the detection solid angle, (4) the fraction of energy dependent self absorption, and (5) the fraction of activity lost in sample preparation. Since the uncertainty in (5) at this stage is far more than the sum of the other factors together, an approximation of their product is obtained by multiplying reasonable estimates of (1)–(4) by an admittedly crude estimate of (5). Thus (1) the efficiency is about 0.6 with $\varepsilon_{609}/\varepsilon_{351}=0.84$ (estimated from stopping power of Ge),[33] (2) the branching ratios are 0.376 and 0.461 to the 609 and 351 keV, respectively,[34] (3) the solid angle is less than 0.5 (2π of total 4π), (4) the self-absorption of the two gamma rays in question through the 1–2 cm thick sample was inconsequential, and (5) was crudely estimated to be 0.5–0.8, yielding a product of less than 6%–10% of the total activity in the sample at the time of measurement and at most about 3%–5% of the activity present when the sample was in secular equilibrium (see Sec. II).

IV. DATA AND ANALYSES

Figures 8–11 show data sets under different meteorological conditions, different preparation times, and with different ages. Figures 8 and 9 show data and fits for samples taken within 2 h during a thunderstorm of 24 May 2006. The activities for the 352 keV line of ^{214}Pb and the 609 keV line of ^{214}Bi are shown as the solid and open circles respectively, with least-squares fitting to Eqs. (1) and (5) as the dashed and solid lines, respectively. The error bars shown reflect relative errors due exclusively to counting statistics. Since both activities are from the same sample and thus prepared and measured in the same manner, the systematic and absolute errors are identical for both curves. This was a heavy thunderstorm with rain rates of about 40 mm/h and thus considerable initial activity resulting in about 10 000 counts in each of the relevant peaks within a 5 min interval, giving rise to statistically significant data. It is noteworthy that both samples shown are consistent with activity accreted during formation in secular equilibrium (see Fig. 2) as are all of the 24 most significant data sets measured in 2006–2007. Rainfall rate data were taken in 10 min intervals with a standard cylindrical tip bucket rain gauge.

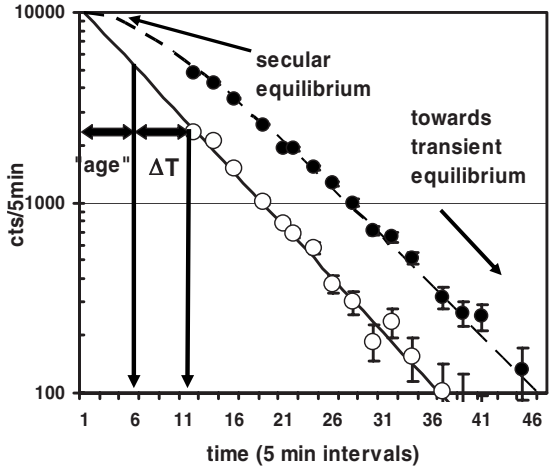

FIG. 10. ^{214}Bi (609 keV closed circles) and ^{214}Pb (352 keV open circles) γ ray count rates as a function of 5.0 min bin collection intervals for a rain sample taken on 2 May 2006, and their theoretical decay curves assuming they are in secular equilibrium at beginning of fall as dashed and solid lines, respectively.

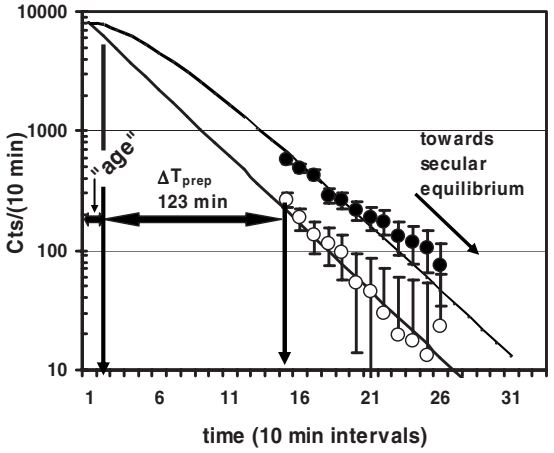

FIG. 11. ^{214}Bi (609 keV closed circles) and ^{214}Pb (352 keV open circles) γ ray count rates as a function of 10.0 min bin collection intervals from a snow sample taken and subsequently melted on 21January 2006, and their theoretical decay curves assuming they are in secular equilibrium at beginning of fall as dashed and solid lines, respectively.

At this point it is not possible to make definitive correlations between rain ages, rainfall rates, and specific cloud heights. Earlier work[1] suggests that it may be reasonable to assume that the concentrations of radon progeny decrease with elevation and are thus largely accreted on the surface of droplets near the base of the cloud. In future work simultaneous data from ceilometers, vertically pointing radar,[35] etc., will be taken in order to better correlate the droplet formation region with ice phase microphysics as well as the extent to which convective currents extending into the upper troposphere correlate with our results. We shall refer to an "effective cloud height" which we will later endeavor to measure, but is herein assumed to account for such features. The mean value of the ages obtained over the 24 most significant data sets was 32.8 min, corresponding to mean velocities from 1.0 ± 0.6 to 2.5 ± 1.5 m s^{-1} for assumed effective cloud heights from 2 to 5 km, respectively, which are in good agreement with the v_{surf} values for the rainfall rates shown in Fig. 5.

The utility of this measurement can be further exemplified in Fig. 10 which shows the activities for the 352 keV line of ^{214}Pb and the 609 keV line of ^{214}Bi as the solid and open circles, respectively, with fits to Eqs. (1) and (5) as the dashed and solid lines, respectively. In this case the initial activity was such that even after 55 min including a preparation delay of 27 min, the activities could still be further tracked for another 3–4 half lives during which time the activity approaches transient equilibrium. Without the fortuitous and experimentally somewhat unique situation, wherein the half lives of ^{214}Pb and ^{214}Bi and the difference between them are on the same scale of time as the rain events being tracked, it would be impossible to make a statistically significant measurement of transition from secular to transient equilibrium.

The extrapolation of the theoretical fits to the data in Figs. 2 and 8–10 provide reliable determinations of GRR at $t=0$ of 8000, 6200, 7100, and 10 000 counts per 5 min, respectively, even though they cannot actually be directly measured. Estimations of the product of the detection efficiency, branching ratios, and percent of total activity concentrated from the collected water yield a product of $\varepsilon_1 b_1 f_1$ of less than 10% [see Eqs. (8)–(10) in Sec. II], and accordingly the above GRRs provide lower limits on the initial activities contained within the rain samples when they were first accreted of 3.2, 0.6, 0.8, and 2.2 Bq l^{-1}, respectively. Knowledge of this activity may be used as a base line for tracing other meteorological processes.

Significant snowfall rates occur infrequently in Tokyo, but it is interesting to note the ages observed during one such event. The activities for the 351 keV line of ^{214}Pb and the 609 keV line of ^{214}Bi are shown in shown in Fig. 11 as the solid and open circles, respectively, with fits to Eqs. (1) and (5) as the dashed and solid lines, respectively, from snow collected on 21 January 2006. In this case fresh snow had to be continuously collected and the preparation time was considerable. The lower age in this case indicates that snow flakes with larger surface area to volume ratios scavenge much of their activity in their journey to ground,[13] and which unlike the activity in rain drops is most likely near secular equilibrium when collected.

Table I shows the range of measured ages from 5 to 101 min with their various errors shown in the third column of the table. The weighted mean age of the data in Table I is 32.8 min. Figure 12 compares the expected average velocity of a unit of surface area of rain verses the transit time that it would take those droplets to fall from the effective cloud heights indicated on the figure. Both the mean weighted ages and their range are consistent with the expected transit times for theoretical surface velocities of about 2–3 m s^{-1}, as shown in Fig. 5. Quite remarkably, all of the ages are consistent with expected transit times for reasonable effective cloud heights and rain drop velocities. The premise that rain ages provide at least lower limits of raindrop transit times is thus verified.

V. SUMMARY AND CONCLUSION

Measurements of relative γ ray activities of ^{214}Bi/^{214}Pb contained in 5–60 l of rain water enabled determination of the age of rain and snow. Since the activities of both radioisotopes were observed within the same sample, by the same detector, and under identical conditions, the only systematic errors were due to the energy dependence of the detection efficiency, relevant branching ratios, and percent of activity gleaned from the sample. These errors could also be eliminated because the two activities began from secular equilibrium where by definition they had a ratio of 1.0 and evolved to transit equilibrium with a ratio of 3.88 within a few half lives (see Eq. (11)), and thus provided two precise theoretical times[28] wherein the ratio of activities could be calibrated. This method has the distinct advantage over most radiometric dating techniques in that the initial activity does not have to be known.

The assumption that the accumulation of γ activity on rain droplets corresponds to the accretion of water during their construction is supported by this work (see Sec. II and Fig. 2) and earlier work.[1,2] This is not unreasonable since the droplet is formed from water containing activity which has

TABLE I. Summary of measured rain ages and source activities.

Date	ΔT_{age} (min)	σT_{age} (min)	Rain (ℓ)	Rate at t_0 count/s	Act at t_0 (count/s ℓ)	σact at t_0 (count/s ℓ)
7/15/06	29	14.8	30	12.9	1.72	1.42
8/12/06	14	6.42	30	11.9	1.59	2.50
8/12/06	15	10.4	30	13.9	1.85	3.59
8/17/06	27	1.80	30	3.98	0.53	0.06
9/1/06	58	15.6	20	22.5	4.50	1.63
9/6/06	30	13.2	20	13.8	2.76	2.30
9/8/06	5.0	1.11	30	13.9	1.85	2.25
9/12/06	52	41.3	30	28.2	3.76	4.48
9/26/06	94	43.4	30	53.6	7.15	4.56
9/26/06	18	6.17	30	7.6	1.01	0.68
11/15/06	64	12.3	30	47.4	6.32	1.88
11/19/06	101	4.11	20	65.4	13.1	0.66
12/13/06	64	33.8	10	23.8	9.52	6.84
12/26/06	34	19.5	30	15.2	2.03	1.85
12/26/06	33	3.96	30	11.9	1.59	0.29
1/6/07	21	16.5	20	8.45	1.69	2.34
2/14/07	7.0	2.13	60	19.3	1.29	1.30
3/15/07	17	4.50	30	5.57	0.74	0.40
4/9/07	18	3.60	30	17.1	2.28	0.90
4/11/07	22	3.67	10	10.6	4.24	1.17
4/16/07	88	12.1	10	21.8	8.72	1.39
4/17/07	76	35.5	20	39.2	7.84	4.44
4/17/07	77	11.7	20	19.4	3.88	0.76
4/28/07	14	6.94	30	21.4	2.85	1.24

had sufficient time to attain to secular equilibrium with its surroundings and since the proportion of the droplet acquired in its formation is likely to be more than it scavenges during its descent. In addition the age of a droplet (tens of minutes) is most likely much less than its gestation period.[2] Verification of this assumption enables one to obtain an estimate of the average transit time for rain. Typical rain ages of tens of min were consistent and reproducible within a given rain event even though the sample collection and preparation time varied from about 20 to 40 min. Comparison of rain drop velocities estimated from the speed it would take a unit surface of rain to fall from a few kilometers within its measured age agrees well with those calculated from velocity and drop size distributions (see Sec. II and Figs. 1, 3–5, and 12).[3–12,20–28,30]

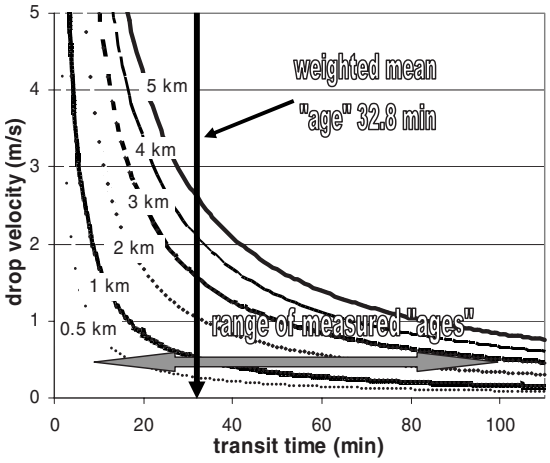

FIG. 12. Average drop surface velocity vs transit time for various effective (see text) cloud heights. Double headed arrow shows extent of age measurements and vertical line shows mean of age measurements.

From extrapolations of fits of the data obtained herein to the theoretical curves of Eqs. (1) and (5) to time $t=0$ (see Figs. 2 and 8–10) realistic estimates of the activity contained in rain before it begins its descent may be obtained (see columns 6 and 7 of Table I). These may then be used for further meteorological studies[36] of cloud formation, precipitation,[14,15] and even lightning,[36] using radon progeny as tracers. Since the source of tracer activity is natural, the process of collecting, condensing, and measuring the activity is relatively simple, fast, and inexpensive;, further application of this method should become a very practical and viable tool for learning about the formation and evolution of precipitation. Further measurements to better correlate ages with precipitation rates,[14,15,37] effective cloud heights,[35] and cloud activities under various meteorological conditions[38] are in progress. The applications of this method, the data obtained, and its theoretical implications are unlimited.

ACKNOWLEDGEMENTS

We thank Professor S. Y. van de Werf, Dr. R. Hazama, Professor G. Austin, Professor D. Krofcheck, Professor P. Barker, Ms. M. Peace, and Ms. S. Greenfield for their comments and support. We would also like to thank the Low Level Radioactivity Laboratory, Auckland University Physics Department, Florida State University Meteorology Department, Florida State University Physics Department, University of Florida Lightning Research Group, Utsunomiya

University, and University of Victoria Physics Department, for hosting one of us (M.G.) during parts of this work. This work was funded in part by the Center of Excellence Grant of ICU.

[1]M. B. Greenfield, A. T. Domondon, S. Tsuchiya, and M. Tomiyama, J. Appl. Phys. **93**, 5733 (2003); M. B. Greenfield, A. T. Domondon, S. Tsuchiya, and M. Tomiyama, *Applications of Accelerators in Research and Industry* (American Institute of Physics, New York, 2003), pp. 820–825.
[2]N. Bhandari and J. Rama, J. Geophys. Res. **68**, 1959 (1963).
[3]R. C. Grosh, Proceedings of the 26th Conference on Radar Meteorology, (AMS, Boston, 1996), pp. 607–610.
[4]R. S. Sekhon and R. C. Srivista, J. Atmos. Sci. **28**, 983 (1971).
[5]A. C. Best, Q. J. R. Meteorol. Soc. **76**, 303 (1950).
[6]E. E. Gossard, R. G. Strauch, D. C. Welsh, and S. Y. Matrosov, J. Atmos. Ocean. Technol. **9**, 108 (1992).
[7]J. H. van Boxel, Workshop on Wind and Water Erosion, 1997 (unpublished) pp. 77–85.
[8]W. G. Uplinger, Proceedings of the Radar Meteorology Conference (AMS, Boston, 1977), pp. 389–391.
[9]R. Gunn and R. D. Kinzer, J. Meteorol. **8**, 249 (1949).
[10]K. V. Beard and H. R. Prupacher, J. Atmos. Sci. **26**, 1066 (1969).
[11]D. Hauser, P. Amayenc, B. Nutten, and P. Wldteufel, J. Atmos. Ocean. Technol. **1**, 256 (1984).
[12]S. Atlas, R. Srivastava, and R. Sekhon, Rev. Geophys. Space Phys. **11**, 1 (1973).
[13]M. B. Greenfield, A. T. Domonodon, N. Okamoto, and I. Watanabe, J. Appl. Phys. **91**, 1628 (2002); Proceedings of the Seventh International Conference on Applications of Nuclear Techniques (World Scientific, Singapore, 2001).
[14]M. B. Greenfield, G. Austin, P. Barker, W. Cottrill, M. Ishigaki, D. Krofcheck, K. Kubo, M. Peace, P. Ruscher, and W. Cottrill, *NZIP Conference Proceedings* (University of Auckland, Auckland, NZ., 2005).
[15]P. Ruscher and W. Cottrill, Florida State University, Department of Meteorology; K. J. Rambo, University of Florida Lightning Center.
[16]J. E. McDonald, J. Meteorol. **11**, 478 (1954).
[17]K. V. Beard, R. J. Kubesh, and H. T. Ochs, J. Atmos. Sci. **48**, 698 (1991).
[18]K. V. Beard and R. J. Kubesh, J. Atmos. Sci. **48**, 2245 (1991).
[19]R. C. Srivastava, J. Atmos. Sci. **28**, 410 (1971).
[20]E. E. Gossard, R. O. Strauch, and R. R. Rogers, J. Atmos. Ocean. Technol. **7**, 815 (1990).
[21]D. Hauser and P. Amenyenc, Radio Sci. **19**, 185 (1984).
[22]J. O. Laws and D. A. Parsons, Trans., Am. Geophys. Union **24**, 452 (1943).
[23]J. Lavergnat and P. Gole, J. Appl. Meteorol. **37**, 805 (1998).
[24]D. Atlas and C. Ulbrich, J. Appl. Meteorol. **16**, 1322 (1977).
[25]J. S. Marshall and W. M. Palmer, J. Meteorol. **5**, 165 (1948); Trans., Am. Geophys. Union **24**, 452 (1948).
[26]C. Richter and M. Hagen, Q. J. R. Meteorol. Soc. **123**, 2277 (1997).
[27]A. C. Best, Q. J. R. Meteorol. Soc. **76**, 302 (1950).
[28]H. Bateman, Proc. Cambridge Philos. Soc. **16**, 423 (1910).
[29]H. D. Young and R. A. Friedman, *University Physics* (Addison-Wesley, New York, 1988).
[30]O. Peters, C. Herlein, and K. Christensen, Phys. Rev. Lett. **88**, 018701 (2001).
[31]K. Komura, Y. Kuwahara, T. Abe, K. Tanaka, Y. Murata, and M. Inoue, J. Radioanal. Nucl. Chem. **269**, 511 (2006).
[32]ORTEC HPGe "Detective," see http://www.ortec-online.com/pdf/detective.pdf
[33]*CRC Handbook of Chemistry and Physics*, 76th ed., edited by D. R. Lide (CRC, New York, 1995), pp. 10–284.
[34]R. B. Firestone and L. P. Ekström, LBNL Isotopes Project, Version 2.1, LUNDS Universiteit, 2004, see http://ie.lbl.gov/toi/
[35]M. B. Greenfield, G. Austin, P. Barker, W. Cottrill, M. Ishigaki, N. Ito, A. Iwata, K. Komura, D. Krofcheck, K. Kubo, M. Peace, P. Ruscher, and P. Smith (unpublished).
[36]S. Miyamoto, H. Kugii, K. Fushimi, C. Hara, N. Koori, T. Korenaga, A. Murata, and S. Nakayama, *Report of Faculty of Integrated Arts and Sciences* (University Tokushima, 2002), Vol. 10, pp. 1–8.
[37]M. B. Greenfield, A. T. Domondon, S. Tsuchiya, K. Kubo, Y. Ikeda, and M. Tomiyama, J. Appl. Phys. **93**, 1839 (2003).
[38]J. Mercier, B. Tracy, R. d'Amours, F. Chagnon, I. Hoffman, E. P. Korpach, S. Johnson, and K. Ungar, Preprint Radiation Protection Bureau of Health Canada, Ottawa (unpublished).